



HAL
open science

Multimodal neuroimaging provides a highly consistent picture of energy metabolism, validating ^{31}P MRS for measuring brain ATP synthesis

M. Chaumeil, J. Valette, M. Guillermier, E. Brouillet, F. Boumezbeur, A.-S. Herard, G. Bloch, P. Hantraye, V. Lebon

► To cite this version:

M. Chaumeil, J. Valette, M. Guillermier, E. Brouillet, F. Boumezbeur, et al.. Multimodal neuroimaging provides a highly consistent picture of energy metabolism, validating ^{31}P MRS for measuring brain ATP synthesis. *Proceedings of the National Academy of Sciences of the United States of America*, 2009, 106 (10), pp.3988-3993. 10.1073/pnas.0806516106 . hal-02155689

HAL Id: hal-02155689

<https://hal.science/hal-02155689>

Submitted on 17 Sep 2019

HAL is a multi-disciplinary open access archive for the deposit and dissemination of scientific research documents, whether they are published or not. The documents may come from teaching and research institutions in France or abroad, or from public or private research centers.

L'archive ouverte pluridisciplinaire **HAL**, est destinée au dépôt et à la diffusion de documents scientifiques de niveau recherche, publiés ou non, émanant des établissements d'enseignement et de recherche français ou étrangers, des laboratoires publics ou privés.

Multimodal neuroimaging provides a highly consistent picture of energy metabolism, validating ^{31}P MRS for measuring brain ATP synthesis

Myriam M. Chaumeil^a, Julien Valette^a, Martine Guillemier^b, Emmanuel Brouillet^b, Fawzi Boumezbeur^a, Anne-Sophie Herard^{a,b}, Gilles Bloch^{a,c}, Philippe Hantraye^{a,b}, and Vincent Lebon^{a,c,1}

^aCommissariat à l'Énergie Atomique (CEA)-I2BM-Medical Imaging Research Center (MIRcen), and ^bCentre National de la Recherche Scientifique-Unité de Recherche Associée 2210-MIRcen, 92265 Fontenay-aux-Roses, France; and ^cCEA-I2BM-NeuroSpin, 91191 Gif-sur-Yvette, France

Edited by Robert G. Shulman, Yale University, New Haven, CT, and approved December 22, 2008 (received for review July 10, 2008)

Neuroimaging methods have considerably developed over the last decades and offer various noninvasive approaches for measuring cerebral metabolic fluxes connected to energy metabolism, including PET and magnetic resonance spectroscopy (MRS). Among these methods, ^{31}P MRS has the particularity and advantage to directly measure cerebral ATP synthesis without injection of labeled precursor. However, this approach is methodologically challenging, and further validation studies are required to establish ^{31}P MRS as a robust method to measure brain energy synthesis. In the present study, we performed a multimodal imaging study based on the combination of 3 neuroimaging techniques, which allowed us to obtain an integrated picture of brain energy metabolism and, at the same time, to validate the saturation transfer ^{31}P MRS method as a quantitative measurement of brain ATP synthesis. A total of 29 imaging sessions were conducted to measure glucose consumption (CMRglc), TCA cycle flux (V_{TCA}), and the rate of ATP synthesis (V_{ATP}) in primate monkeys by using ^{18}F -FDG PET scan, indirect ^{13}C MRS, and saturation transfer ^{31}P MRS, respectively. These 3 complementary measurements were performed within the exact same area of the brain under identical physiological conditions, leading to: $\text{CMRglc} = 0.27 \pm 0.07 \mu\text{mol}\cdot\text{g}^{-1}\cdot\text{min}^{-1}$, $V_{\text{TCA}} = 0.63 \pm 0.12 \mu\text{mol}\cdot\text{g}^{-1}\cdot\text{min}^{-1}$, and $V_{\text{ATP}} = 7.8 \pm 2.3 \mu\text{mol}\cdot\text{g}^{-1}\cdot\text{min}^{-1}$. The consistency of these 3 fluxes with literature and, more interestingly, one with each other, demonstrates the robustness of saturation transfer ^{31}P MRS for directly evaluating ATP synthesis in the living brain.

glycolysis | TCA cycle | oxidative phosphorylation | NMR spectroscopy | metabolic fluxes

Numerous brain disorders, like neurodegenerative diseases, are associated with impairment in energy metabolism. This observation has been driving considerable technological developments in medical imaging, aiming at measuring brain energy metabolism. PET combined with ^{18}F -2-fluoro-2-deoxy-D-glucose (^{18}F -FDG) injection has been used in research on normal and pathological brain for ≈ 30 years (1–3). More recently, magnetic resonance spectroscopy (MRS) has brought new tools for imaging cerebral energy fluxes (4–16).

However, methodological developments are still needed to answer the clinical need for earlier diagnosis and follow-up of neurodegenerative pathologies. Although PET detection of ^{18}F -FDG has proven efficient to map cerebral glucose consumption (CMRglc), this technique does not directly reflect energy storage and utilization that is mainly derived from glucose oxidation. Also, PET is unlikely to become widely accessible, due to its invasiveness and cost. However, magnetic resonance is of widespread use for anatomical imaging, and clinical scanners can be equipped for metabolic imaging at limited cost. Indeed, MRS has proven powerful to measure brain energy metabolism by detecting ^{13}C , ^{17}O , or ^{31}P nuclei, which only require dedicated radiofrequency components. Quantitative measurement of cerebral oxidative metabolism by ^{13}C (4–11) or ^{17}O (14–16) MRS

has been demonstrated. However, these approaches require i.v. injection of expensive precursors followed by time-consuming acquisition. In contrast, ^{31}P MRS has the potential to measure the cerebral rate of ATP synthesis V_{ATP} without any injection, using the magnetization transfer technique as originally demonstrated by Brown *et al.* (17). Up to now, only 2 measurements of cerebral V_{ATP} have been reported in rodents (12, 18), and 1 in humans (13). MRS-derived V_{ATP} reported in these pioneer studies appeared consistent with literature values and coupled with brain activity over a large range of anesthesia (18). However, MRS-derived V_{ATP} may be contaminated by a near-equilibrium exchange reaction between inorganic phosphate (P_i) and ATP catalyzed by the glycolytic enzymes GAPDH and phosphoglycerate kinase (PGK). Such a contamination, leading to an overestimation of the NMR-detected V_{ATP} , was inconsistently reported on yeast suspensions (19), with a possible dependence on the growth medium. MRS-derived V_{ATP} was also shown to be contaminated by glycolytic enzymes *ex vivo* on perfused peripheral organs (20, 21), on rodent skeletal muscle (22), and human skeletal muscle (23). Given these elements, further studies are required to establish ^{31}P magnetization transfer as a reliable quantitative method for measuring the cerebral rate of energy synthesis V_{ATP} .

In this context, our purpose has been to validate the ^{31}P MRS measurement of brain V_{ATP} , by comparing the rate of ATP synthesis measured in primates with CMRglc and TCA cycle rate (V_{TCA}) measured by PET and ^{13}C MRS, respectively. Under normal physiological conditions, glucose breakdown (through glycolysis and TCA cycle) is stoichiometry coupled to ATP synthesis, so that theoretical V_{ATP} can be calculated from the measured CMRglc and V_{TCA} , providing a direct way to validate MRS-measured V_{ATP} .

Results show that CMRglc and V_{TCA} measured in the primate brain are highly consistent, showing the expected 1:2 stoichiometry between glycolysis and TCA cycle (1 glucose giving rise to 2 pyruvate molecules). Also, the theoretical value of V_{ATP} derived from CMRglc and V_{TCA} is very close to that directly measured using ^{31}P MRS and magnetization transfer. These results demonstrate that ^{31}P MRS is a reliable method to measure brain ATP synthesis *in vivo*.

Results

High-resolution scout MRI of the monkey brain is presented on Fig. 1, showing the 8-mL volume of interest (VOI) where the 3

Author contributions: E.B., G.B., P.H., and V.L. designed research; M.M.C., J.V., M.G., F.B., and A.-S.H. performed research; M.M.C. and J.V. analyzed data; and M.M.C., E.B., and V.L. wrote the paper.

The authors declare no conflict of interest.

This article is a PNAS Direct Submission.

Freely available online through the PNAS open access option.

¹To whom correspondence should be addressed. E-mail: vincent.lebon@cea.fr.

© 2009 by The National Academy of Sciences of the USA

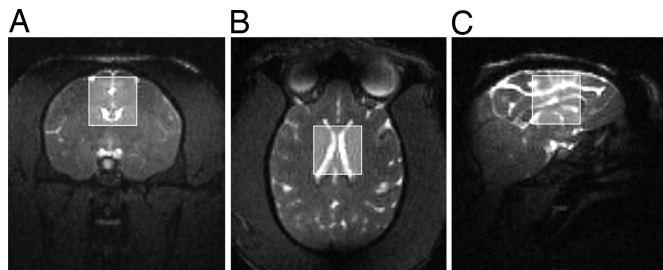


Fig. 1. Three-dimensional MRI images acquired in 1 monkey. The position of the VOI in which CMRglc, V_{TCA} , and V_{ATP} were measured is presented on coronal (A), axial (B), and sagittal images (C).

metabolic fluxes were measured. Anatomical landmarks on coronal, axial, and sagittal images made it possible to reposition the VOI identically for all imaging sessions.

A typical ^{18}F -FDG PET image (axial view; acquisition time, 20 min) is presented on Fig. 2A. The corresponding ^{18}F time activity curve in the selected VOI and the experimental ^{18}F arterial time activity curve are plotted in Fig. 2B. Kinetic analysis of ^{18}F -FDG uptake produced an estimation of ^{18}F -FDG-6-P and ^{18}F -FDG contributions to total activity (Fig. 2B), leading to $CMRglc = 0.27 \pm 0.07 \mu\text{mol}\cdot\text{g}^{-1}\cdot\text{min}^{-1}$.

Fig. 3A shows a stacked plot of difference $^1H\{-^{13}C\}$ spectra (averaged over the 8 ^{13}C NMR sessions) acquired during an i.v. infusion of $[U\text{-}^{13}C_6]$ glucose. Corresponding ^{13}C -enrichment time courses of glutamate C3 and C4 are presented in Fig. 3B. The continuous lines represent the best fit to experimental data according to the metabolic model. This analysis leads to $V_{TCA} = 0.63 \pm 0.12 \mu\text{mol}\cdot\text{g}^{-1}\cdot\text{min}^{-1}$.

The P_i region of ^{31}P spectra acquired with γ -ATP saturation for 4 different saturation times (0.5, 1.0, 1.5, and 2 s) is presented in Fig. 4A (averaged over the 15 ^{31}P NMR sessions). It shows that P_i amplitude is decreased while the saturation time is increased. Note that P_i decrease on this figure is due to both saturation transfer effect and RF bleed over effect, the later explaining the decrease of resonances surrounding P_i (mostly phosphodiester and phosphomonoesters ≈ 3 and 7 ppm, respectively); ^{31}P spectra were corrected for RF bleed over by subtracting γ -ATP saturated spectra from control spectra where saturation was applied symmetrically to γ -ATP. Inversion-recovery experiments yielded a mean value of $TI^{mix} = 2.05$ s. Consequently, the averaged P_i attenuation vs. t_{sat} was fitted fixing the following parameters: $TI^{mix} = 2.05$ s, $\theta = 60^\circ$, $TR = 2.95$ s. The best fit is shown on Fig. 4B. The estimation of k_f and TI^{int} from averaged $M_S(t_{sat})/M_C(t_{sat})$ fitting and Monte Carlo simulation yielded $k_f =$

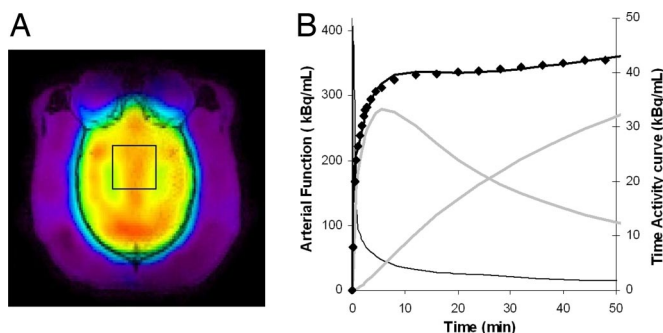


Fig. 2. CMRglc measurement by ^{18}F PET. (A) VOI from which the total ^{18}F activity was extracted, (B) corresponding ^{18}F -FDG PET time-activity curve (\blacklozenge) and best fit by the 2-tissue compartment model (bold solid line). Arterial function measured in the same session is presented (thin solid line). Modeled contributions of ^{18}F -FDG and ^{18}F -FDG-6-P are shown (gray lines).

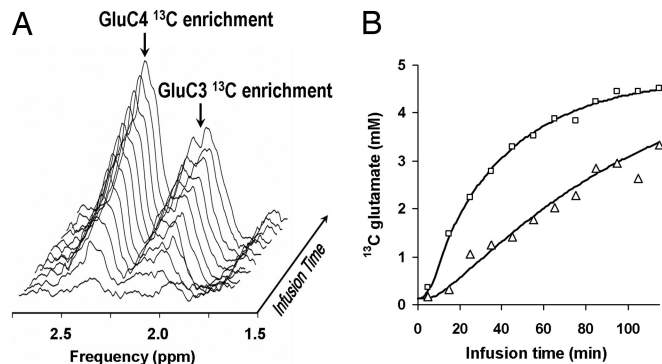


Fig. 3. V_{TCA} measurement by indirect ^{13}C NMR. (A) Stack plot of $^1H\{-^{13}C\}$ difference spectra in glutamate C3 and C4 region. Glutamate ^{13}C enrichment appears at the frequency of C3 and C4 mother resonances on our 1H difference spectra. Spectra were post processed by a 5 Hz lorentzian line broadening. (B) ^{13}C enrichments time courses (averaged over 8 sessions) measured for glutamate C3 (Δ), glutamate C4 (\square), and best fit to the data (solid lines).

$0.10 \pm 0.03 \text{ s}^{-1}$ and $TI^{int} = 2.1 \pm 0.4$ s. Cerebral P_i concentration was fixed to $[P_i] = 1.3$ mM, according to literature values (24–29). By using a brain density of 1g/mL, we obtained the ATP synthesis rate $V_{ATP} = 7.8 \pm 2.3 \mu\text{mol}\cdot\text{g}^{-1}\cdot\text{min}^{-1}$.

The 3 metabolic fluxes measured in this study and their metabolic couplings are presented on Fig. 5.

Discussion

Consistency of Each Measured Flux with Literature Values. Taken independently, the CMRglc and V_{TCA} fluxes measured in this study are consistent with literature values of brain energy metabolism for anesthetized animals (30–33), and particularly with the values reported by Boumezbeur *et al.* (30) in the monkey brain ($CMRglc = 0.23 \pm 0.03 \mu\text{mol}\cdot\text{g}^{-1}\cdot\text{min}^{-1}$; $V_{TCA} = 0.53 \pm 0.13 \mu\text{mol}\cdot\text{g}^{-1}\cdot\text{min}^{-1}$). The small differences between these values and CMRglc and V_{TCA} measured in this study could be explained by differences in VOI position, and consequently by different contributions of gray and white matter to the detected fluxes: in our study, gray matter accounts for $58 \pm 2\%$ of the detected brain tissue, as measured on high resolution $T1$ -weighted images (data not shown). This percentage is likely to be higher than gray matter content in the voxel detected by Boumezbeur *et al.* (30), which was located deeper in the brain and included significantly less cortical areas. Given the strong de-

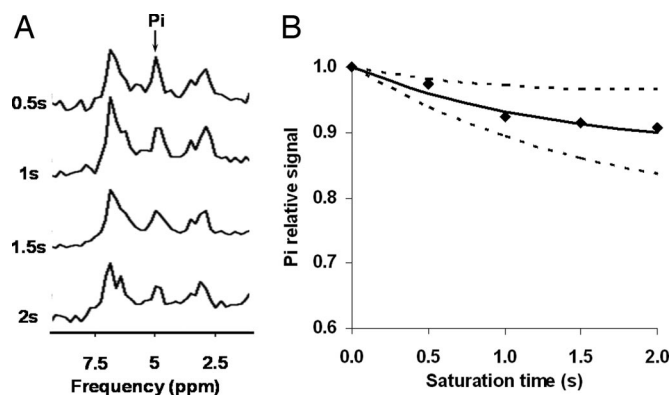


Fig. 4. V_{ATP} measurement by ^{31}P saturation transfer NMR. (A) P_i region of ^{31}P spectra acquired on γ -ATP saturation for 4 different saturation times (0.5, 1.0, 1.5, and 2 s). P_i amplitude decreases as saturation time is increased. (B) P_i attenuation $[M_S(t_{sat})/M_C(t_{sat})]$ vs. saturation time t_{sat} . The solid line is the best fit to experimental P_i attenuation (\blacklozenge). The dotted lines indicate the lower and upper limits of the fit based on k_f and TI^{int} SD.

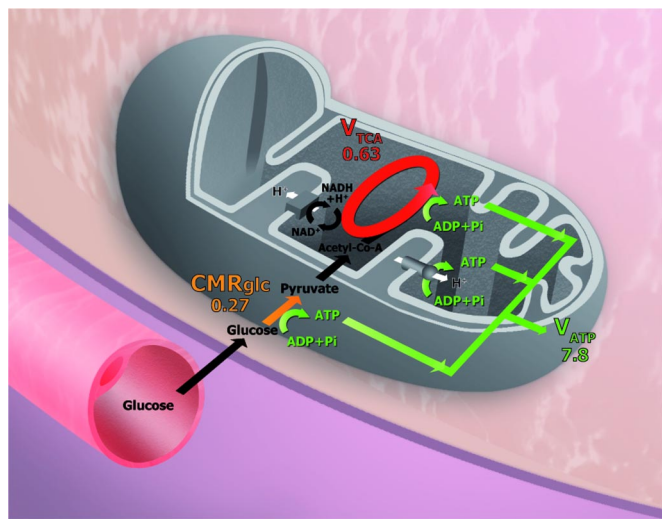


Fig. 5. Brain energy metabolism as measured by multimodal imaging: ^{18}F -FDG was used to quantify CMRglc, ^{13}C MRS was used to measure V_{TCA} , and ^{31}P MRS was used to measure V_{ATP} . The 3 fluxes are highly consistent, validating ^{31}P MRS as a robust tool for quantifying brain ATP synthesis.

pendence of glucose metabolism on gray matter content (7), a slight difference in gray matter fraction might explain our higher CMRglc and V_{TCA} values (0.27 and $0.63 \mu\text{mol}\cdot\text{g}^{-1}\cdot\text{min}^{-1}$, respectively). PET measurements of CMRglc have been reported recently in the monkey brain, and found to be close to $0.3 \mu\text{mol}\cdot\text{g}^{-1}\cdot\text{min}^{-1}$ in brain areas similar to our VOI (31). This value is very close to our measurement ($0.27 \mu\text{mol}\cdot\text{g}^{-1}\cdot\text{min}^{-1}$).

Our V_{TCA} values ($0.63 \pm 0.12 \mu\text{mol}\cdot\text{g}^{-1}\cdot\text{min}^{-1}$) are in agreement with reported human values that range from 0.57 to $0.77 \mu\text{mol}\cdot\text{g}^{-1}\cdot\text{min}^{-1}$ (6, 8, 9, 11).

The measurement of V_{ATP} reported in this article is, to our knowledge, the first one performed in the monkey brain. Compared with the only one reported measurement of cerebral V_{ATP} that was performed in humans (13), the V_{ATP} value reported in this study appears slightly lower ($7.8 \pm 2.3 \mu\text{mol}\cdot\text{g}^{-1}\cdot\text{min}^{-1}$ vs. $12.1 \pm 2.8 \mu\text{mol}\cdot\text{g}^{-1}\cdot\text{min}^{-1}$). However, the SD ranges of both measurements overlap so that no significant difference can be inferred.

Consistency Between CMRglc and V_{TCA} . In this study, a [V_{TCA} /CMRglc] ratio of 2.25 is measured, reflecting the metabolic coupling between glycolysis and TCA cycle. Considering that glucose is the unique metabolic fuel under normal physiological conditions, a [V_{TCA} /CMRglc] ratio of 2 would be expected, because glycolysis produces 2 molecules of pyruvate per glucose. The measured [V_{TCA} /CMRglc] ratio is 12.5% higher than the expected theoretical value, leaving room for a possible contribution of fatty acids to the TCA cycle ($\text{CMR}_{\text{FA}} = V_{\text{TCA}} - 2 \text{CMRglc}$). However, given the fact that the SD on each flux (V_{TCA} and CMRglc) is $\approx 15\%$, the [V_{TCA} /CMRglc] ratio is not high enough to claim a significant contribution of the fatty acid pathway. The 12.5% excess over theoretical ratio could be partly ascribed to experimental inaccuracy.

Potential Effect of Glycemia on the Measured Fluxes. Blood glucose was measured during the course of PET and ^{13}C -NMR sessions. Glycemia measured at the beginning of ^{13}C -NMR sessions (before ^{13}C glucose injection) and during the course of PET measurements were all in the $3\text{--}5 \text{mmol}\cdot\text{L}^{-1}$ normoglycemic range; ^{13}C measurement of V_{TCA} was performed under hyperglycemia ($9\text{--}15 \text{mmol}\cdot\text{L}^{-1}$ in our study), because a several fold increase in glycemia is required to bring ^{13}C enrichment of blood

glucose up to $>50\%$. In this context, one may wonder whether CMRglc and V_{TCA} are affected by blood glucose content. CMRglc dependence on glycemia has been studied by several groups, who concluded that brain glucose uptake is not affected by acute hyperglycemia. Evidence for this result was demonstrated in rodents as well as in humans (34, 35). Unfortunately, V_{TCA} dependence on glycemia has not been studied as thoroughly as CMRglc, due to the lack of method (besides ^{13}C NMR) for noninvasive measurement of the TCA cycle flux. It must be kept in mind that V_{TCA} measured using ^{13}C -labeled glucose includes the contributions of all possible substrates of acetyl-CoA oxidation. Therefore, NMR-measured V_{TCA} is directly coupled to CMRO_2 (14), as shown *ex vivo* on brain slices (36). Since several studies have reported that CMRO_2 remains independent from glycemia in mammals (37, 38), the absence of glycemic dependence can be reasonably extended to V_{TCA} . Note that glycemia was not measured during ^{31}P -NMR sessions, because V_{ATP} measurement does not require vascular catheterization. Due to the similarity of experimental conditions with PET and preinfusion ^{13}C -NMR sessions, it can be reasonably considered that V_{ATP} was measured under normoglycemia. Given these elements, one can assume that the metabolic fluxes measured in our study were not noticeably affected by glycemic differences.

Validation of V_{ATP} as Measured by NMR. Given the values of CMRglc and V_{TCA} , the corresponding ATP synthesis rate V_{ATP} can be theoretically expressed by establishing stoichiometry between molecules of ATP and reducing equivalents (*i*) generated by the TCA cycle and oxidative phosphorylation, (*ii*) generated by glycolysis, and (*iii*) consumed by the fatty acid pathway. It is well known that the degradation of 1 acetyl-CoA in the TCA cycle leads to the production of 1 ATP, 3 NADH,H^+ , and 1 FADH_2 , and that glycolysis leads to the production of 2 pyruvate, 2 ATP, and 2 NADH,H^+ , a posteriori transformed in 2 FADH_2 by crossing the mitochondrial membrane. Also, the conversion of pyruvate into acetyl-CoA in the mitochondrial matrix leads to the production of 2 NADH,H^+ . Under the hypothesis of all pyruvates produced through glycolysis being converted into acetyl-CoA, the rate of this reaction can be assumed to be equal to CMRglc. Then, the corresponding V_{ATP} can be expressed as:

$$V_{\text{ATP}}^{\text{TH}} = (2(P/O)_{\text{FADH}_2} + 2(P/O)_{\text{NADH},\text{H}^+} + 2) \text{CMRglc} + (3(P/O)_{\text{NADH},\text{H}^+} + (P/O)_{\text{FADH}_2} + 1) V_{\text{TCA}} - \text{CMR}_{\text{FA}} \quad [1]$$

where $(P/O)_{\text{NADH},\text{H}^+}$ and $(P/O)_{\text{FADH}_2}$ are the number of ATP molecules per atom of oxygen produced by the degradation of 1 NADH,H^+ and 1 FADH_2 , respectively, in the respiratory channel. Based on established values for the P/O ratios [$(P/O)_{\text{NADH},\text{H}^+} = 2.3$ and $(P/O)_{\text{FADH}_2} = 1.4$; see ref. 39], the theoretical rate of ATP synthesis expected from the rate of CMRglc and V_{TCA} we measured in the present study was: $V_{\text{ATP}}^{\text{TH}} = 8.3 \pm 1.8 \mu\text{mol}\cdot\text{g}^{-1}\cdot\text{min}^{-1}$. This value is very close to the NMR-measured V_{ATP} ($7.8 \pm 2.3 \mu\text{mol}\cdot\text{g}^{-1}\cdot\text{min}^{-1}$). The slightly lower measured value could be explained by a partial uncoupling between the generation of the proton gradient and the use of this gradient for synthesis of ATP from ADP and P_i . Possible explanation for partial uncoupling might involve specific uncoupling proteins like the brain-specific UCP4 (40, 41). However, the theoretical expected value $V_{\text{ATP}}^{\text{TH}}$ is well within the measurement error of our ^{31}P -NMR measured V_{ATP} . Therefore, our study does not allow us to conclude on significant uncoupling process in the mammal brain.

To our knowledge, only one previous study was performed in humans to assess the coupling between V_{TCA} and V_{ATP} , measured by ^{13}C NMR and ^{31}P NMR, respectively (23). This study, performed in skeletal muscle, reported the following values:

$V_{TCA} = 0.06 \mu\text{mol}\cdot\text{g}^{-1}\cdot\text{min}^{-1}$ and $V_{ATP} \approx 5 \mu\text{mol}\cdot\text{g}^{-1}\cdot\text{min}^{-1}$. According to Eq. 1, the theoretical value of V_{ATP} expected from the measured V_{TCA} ranges from $V_{ATP}^{TH} = 0.5 \mu\text{mol}\cdot\text{g}^{-1}\cdot\text{min}^{-1}$ (assuming that FA is the sole substrate for muscle, i.e., $\text{CMR}_{\text{glc}} = 0$ and $\text{CMR}_{\text{FA}} = \frac{1}{2}V_{TCA}$) to $V_{ATP}^{TH} = 0.8 \mu\text{mol}\cdot\text{g}^{-1}\cdot\text{min}^{-1}$ (assuming that glucose is the sole substrate, i.e., $\text{CMR}_{\text{glc}} = \frac{1}{2}V_{TCA}$ and $\text{CMR}_{\text{FA}} = 0$). Thus, the range of expected V_{ATP}^{TH} values is 10 to 6 times as low as ^{31}P -NMR measured V_{ATP} ($\approx 5 \mu\text{mol}\cdot\text{g}^{-1}\cdot\text{min}^{-1}$), which demonstrates that the GADPH shunting is dominant in human skeletal muscle. In contrast, the present study gives a cerebral V_{ATP} slightly lower than the theoretical value expected from CMR_{glc} and V_{TCA} ; thus, ruling out the possibility of a contribution of reversible synthesis by GADPH/PGK at the glycolytic level in the brain. Our data would be consistent with the fact that P_i is mostly present in neurons while a strong glycolytic component takes place in astrocytes as postulated by Lei *et al.* (13). This explanation relies on the hypothesis that lactate (provided by astrocytes through an astrocyte-neuron lactate shuttle) is the major substrate for neuronal oxidative metabolism. Although experimental evidences argue in favor of lactate shuttle having a key role in glutamatergic activation (42, 43), the significance of this shuttle remains controversial (44, 45). More importantly, the extent of physiological conditions under which the lactate shuttle dominates direct neuronal glucose uptake remains to be explored. It must be kept in mind that the animal and human metabolic fluxes discussed here were measured under light anesthesia or alpha state (peaceful wakefulness). Further studies will be required to establish that lactate shuttle remains predominant under those physiological conditions.

In conclusion, this study is, to our knowledge, the first report of cerebral CMR_{glc} , V_{TCA} , and V_{ATP} measurements in the same animals under identical physiological conditions. This unique multimodal approach allows a cross-validation of the described ^{18}F -FDG, ^{13}C MRS, and ^{31}P MRS techniques. In particular, this is a direct *in vivo* validation of the ^{31}P saturation transfer method as a reliable measurement of the cerebral ATP synthesis rate. Implementation of the 3 methodological approaches brings a unique integrated picture of brain energy metabolism, from glucose phosphorylation to mitochondrial ATP synthesis. This multimodal approach will help to better understand mitochondrial energy defects that are thought to have a key role in neurodegenerative illnesses (46, 47).

Materials and Methods

The study was conducted on 3 healthy male monkeys (*macaca fascicularis*, body weight ≈ 5 kg) after they were fasted overnight. All experimental procedures were performed in strict accordance with the recommendations of the European Community (86/609) and the French National Committee (87/848) for care and use of laboratory animals. For both PET and NMR sessions, animals were identically anesthetized by a single ketamine-xylazine intramuscular injection followed by an *i.v.* infusion of propofol ($\approx 200 \mu\text{g}/\text{kg}/\text{min}$), intubated, and ventilated. The head was placed in the Sphinx position by using a home made stereotaxic frame with bite-bar and ear rods. During NMR and PET sessions, physiological parameters were monitored and remained stable within normal ranges: 35–37 °C for body temperature, 50–60 mm Hg for noninvasive blood pressure as measured with an air-cuff placed around the arm, 90–110 min for cardiac frequency, 18–23 min for respiratory frequency, and 35–40 mm Hg for expired CO_2 saturation.

Experimental Design. Neuroimaging sessions. In this study, the experimental plan aimed at measuring the 3 following metabolic fluxes in a same $2 \times 2 \times 2 \text{ cm}^3$ cerebral VOI on the group of monkeys: (i) CMR_{glc} using PET acquisitions after *i.v.* injection of ^{18}F -FDG (1-h acquisition time, 6 sessions: 2 per monkey); (ii) V_{TCA} using indirect ^{13}C -NMR spectroscopy during an *i.v.* infusion of $[\text{U-}^{13}\text{C}_6]$ glucose (2-h acquisition time, 8 sessions: 2 to 3 per monkey); and (iii) V_{ATP} using ^{31}P -NMR spectroscopic acquisition by saturation transfer (1.40-h acquisition time, 15 sessions: 4 to 6 per monkey). Given the long acquisition time of NMR measurements, animal welfare motivated our decision not to perform ^{13}C -

NMR and ^{31}P -NMR during the same session, and to allow at least 2 weeks recovery between 2 subsequent imaging sessions for each monkey.

Each imaging modality has its own sensitivity to the measured metabolic flux: under our experimental conditions, V_{TCA} determination by ^{13}C NMR was less accurate than CMR_{glc} determination by PET, likely due to the intrinsic low sensitivity of NMR spectroscopy. V_{ATP} determination by ^{31}P NMR was even less accurate than the V_{TCA} determination, mostly due to the high number of measured parameters required to assess V_{ATP} . Our purpose being to compare the 3 fluxes, the number of imaging sessions was empirically set to compensate for sensitivity differences between modalities. This empirical design allowed assessing the 3 fluxes with similar accuracies.

VOI positioning and multimodal registration. Proper comparison of the 3 metabolic fluxes requires reproducible positioning of the VOI in the brain for all imaging sessions. For ^{13}C and ^{31}P NMR sessions, high-resolution 3D MRI images of the brain (gradient echo sequence, matrix $128 \times 128 \times 128$, resolution $1 \times 1 \times 1 \text{ mm}^3$) were acquired to position the 8-mL VOI. Accurate repositioning was easily achieved for each monkey by using anatomical landmarks on coronal, axial, and sagittal images (Fig. 1), so that NMR acquisitions were performed in comparable VOIs. Since PET provided images of the whole brain, it was necessary to localize the 8-mL VOI on PET images to assess CMR_{glc} from this volume only. We registered 3D reconstructed PET images with 3D MRI by using robust and fully automated rigid registration method (48). Registration allowed one to accurately localize the NMR detected VOI within PET images and to extract ^{18}F time activity from this VOI.

CMR_{glc} Measurement by ^{18}F PET. PET sessions. PET experiments were performed on an ECAT EXACT HR+ tomograph (Siemens-CTI). After completing a transmission scan with a ^{68}Ga - ^{68}Ge source for attenuation correction, 24 emission scans (63 slices, 4.5-mm isotropic intrinsic resolution) were collected for 60 min after ^{18}F -FDG *i.v.* bolus injection ($\approx 2.5 \text{ mCi}$). To obtain arterial blood function, blood samples were withdrawn every 15 s during the first 2 min of acquisition; then, at 2.30, 3, 5, 7, 10, 15, 20, 30, 40, and 50 min. Arterial blood radioactivity was measured in a cross-calibrated γ -counter (Cobra Quantum D5003; Perkin-Elmer). For control of physiological stability, measurements of glycemia, blood pH, pO_2 , pCO_2 , sO_2 were performed at the beginning, after 20 min and at the end of the acquisition protocol.

Flux quantification. The 8-mL VOI was extracted from the 24 PET images as described above, and the corresponding time activity curve was generated with regional activity calculated for each frame and plotted vs. time. The time activity curve was then fitted by using a 2-tissue compartment model in PMOD (PMOD Technologies) (49), under the hypothesis of irreversible phosphorylation ($k_4 = 0$). The kinetic constants k_1 , k_2 , and k_3 describing the exchanges between the pools of plasmatic ^{18}F -FDG, cytoplasmic ^{18}F -FDG, and cytoplasmic phosphorylated ^{18}F -FDG-P were derived from this adjustment. The lumped constant (LC) was fixed to 0.42, according to previous studies (30, 31). Last, CMR_{glc} was calculated from the values of glycemia, LC, k_1 , k_2 , and k_3 .

V_{TCA} Measurement by Indirect ^{13}C NMR. NMR setup and voxel positioning. MR experiments were performed on a whole-body 3 Tesla system (Bruker) equipped with a surface coil placed on top of the head (double-tunable ^1H - ^{31}P , $\text{O} \approx 4.5 \text{ cm}$). V_{TCA} sessions started with the acquisition of the 3D MRI and the positioning of the VOI. VOI shimming was performed down to $\approx 8 \text{ Hz}$ by means of the FASTMAP algorithm (50), for first- and second-order shim coils.

Indirect ^{13}C NMR spectroscopy. Spectra were collected by using a ^1H STEAM sequence (TE/TM/TR = 21/110/2500, 256 transients). Additional localization was achieved by a B_1 -Insensitive TRain to Obliterate signal (BISTRO) outer volume suppression (OVS) pulse train (51), consisting of 15 modules repeated at increasing RF power levels. Each module was formed by 3 double-band hyperbolic secant pulses selectively saturating slabs outside the $2 \times 2 \times 2 \text{ cm}^3$ VOI along the X, Z, and Y directions (52). OVS was combined with VAPOR water suppression (53). At the beginning of the experiment, a baseline ^1H STEAM spectrum was acquired within the VOI. Then, ^1H STEAM spectra were collected during a 2-step infusion protocol of $[\text{U-}^{13}\text{C}_6]$ glucose. Infusion started with a 3-min bolus of $[\text{U-}^{13}\text{C}_6]$ glucose ($\approx 0.3 \text{ mL}/\text{kg}/\text{min}$, 20% wt/vol), leading quickly to a 3-fold increase in glycemia: blood glucose concentration before bolus infusion was typically $3\text{--}5 \text{ mmol}\cdot\text{L}^{-1}$ and reached $9\text{--}15 \text{ mmol}\cdot\text{L}^{-1}$ after the bolus. Then, a continuous 2-h *i.v.* infusion of a 2:1 mixture of $[\text{U-}^{13}\text{C}_6]$ and unlabeled glucose was performed at lower rate ($\approx 0.01 \text{ mL}/\text{kg}/\text{min}$, 20% wt/vol). This 2-step infusion leads to a stabilization of ^{13}C fractional enrichment (FE) of plasma glucose ≈ 55 to 60% after 5 min and until the end of infusion (52). Control measurements of glycemia were performed by using a Onetouch glucose meter (Lifescan).

Spectra quantification and V_{TCA} measurement. Measurement of ^{13}C -glutamate enrichment from the ^1H spectra was based on a previously described method (30, 52). Briefly, the subtraction of ^1H spectra acquired during the $[\text{U-}^{13}\text{C}_6]$

glucose infusion from the baseline ^1H spectrum results in difference spectra exhibiting only labeled nuclei: mainly glutamate C3 and C4 in the brain; ^{13}C enrichment has 2 effects on the ^1H spectrum: ^1H coupled to ^{13}C (satellite resonance) appear as a doublet, whereas ^1H bound to ^{12}C (mother resonance) decrease. Subtracting a ^{13}C -enriched spectrum from a baseline spectrum provides a difference spectrum where mother resonances exhibit positive intensities (at 2.11 ppm for GluC3 and 2.35 ppm for GluC4), whereas ^{13}C satellite resonances appear antiphased (at 2.85 and 1.85 ppm for GluC4 and at 1.65 and 2.65 ppm for GluC3); ^1H difference spectra collected during ^{13}C -glucose infusion are dominated by changes in mother resonances, as shown on Fig. 3A; ^1H difference spectra were quantified by using Java-based MR user interface (jMRUI; see ref. 54), which performs time domain analysis of free-induction decays. An original basis set of simulated ^1H difference spectra of glutamate C4 and C3 ^{13}C -enrichment was implemented for the quantitation based on quantum estimation algorithm (QUEST; see ref. 55) within jMRUI, by using literature values of resonance frequencies and J-coupling constants (56). The time courses of C4 and C3 enrichment were first estimated. To assess the value of the TCA cycle flux V_{TCA} , a single compartment model describing the incorporation of ^{13}C from blood glucose into brain glutamate was implemented on Matlab (The MathWorks Inc.) (5, 33). The following assumptions were made: (i) glucose transport through the blood-brain barrier follows a reversible Michaelis-Menten kinetic, (ii) the exchange rates V_X between glutamate and α -ketoglutarate and between oxaloacetate and aspartate are equal, (iii) the rate of the glutamate/glutamine cycling is equal to $0.46 \times V_{\text{TCA}}$ (5). The concentrations of glutamate, glutamine, aspartate, lactate, oxaloacetate, and α -ketoglutarate, as well as the glucose transport parameters, were taken from a previous monkey study (52).

V_{ATP} Measurement by ^{31}P Saturation Transfer NMR. NMR setup and voxel positioning. MR experiments were performed on the previously described 3T system equipped with the same surface coil. VOI positioning and shimming were performed the same way as for V_{TCA} sessions.

Theory. Consider the chemical equilibrium between inorganic phosphate P_i and ATP:



where k_f and k_r are the unidirectional rate constants of ATP synthesis and hydrolysis, respectively. To derive the rate of ATP synthesis $V_{\text{ATP}} = k_f[\text{P}_i]$, k_f is measured by progressively saturating the magnetization of γ -ATP and observing the effect on the magnetization of the exchange partner P_i . Then, k_f is derived from the Bloch equations modified for chemical exchange. This method can be applied to ATP synthesis because the lifetime of P_i ($1/k_r$) is in the same order as the intrinsic longitudinal relaxation time of P_i T_1^{int} . This observation explains why the saturation transfer method is specifically sensitive to ATP synthesis, although P_i is involved in several biochemical reactions (12, 13, 17, 18). However, it must be noted that the P_i to ATP conversion catalyzed by the GAPDH/PGK enzymes at the glycolytic level is fast enough to potentially contaminate ^{31}P -NMR measured P_i attenuation (20–23).

Saturation Transfer ^{31}P MRS Experiment. The ^{31}P spectra were collected from the VOI by using an OVS-localized saturation transfer sequence (57). A saturation pulse (variable length t_{sat}) was followed with a BISTRO OVS pulse train (total

OVS train length t_{OVS} , 310 ms). A 100- μs broadpulse was placed immediately after the OVS module for nonselective excitation. The saturation frequency was first set to γ -ATP frequency (-7.35 ppm relative to P_i), and spectra were collected for 4 different values of t_{sat} (0.5, 1.0, 1.5, and 2 s) by using a 2.95-s TR and 512 transients for each t_{sat} . Then, control spectra without γ -ATP saturation were collected. To correct for the RF bleed over effect, control spectra were acquired with a saturation frequency set to $+7.35$ ppm relative to P_i (control saturation symmetric to γ -ATP) for the same 4 values of t_{sat} . The total acquisition time including shimming for each t_{sat} was ≈ 100 min.

Inversion recovery experiment. The T_1 of P_i in the presence of chemical exchange T_1^{mix} was measured by using an inversion recovery sequence: a 180° adiabatic hyperbolic secant pulse (length, 4 ms) set on P_i frequency and a gradient crusher (length, 2 ms) were placed before the OVS module at variable inversion time TI (TI, time between inversion pulse and acquisition). Note that for the TI = 0 experiment, the inversion pulse was placed between the OVS module and the acquisition pulse. Repetition time was fixed to 6.4 s to allow full relaxation of P_i magnetization (T_1^{mix} is expected ≈ 2 s at 3 Tesla); ^{31}P spectra were acquired for 7 values of TI (128 transients).

Spectra quantification. All ^{31}P spectra were zero-filled to 2,048 points and analyzed by using an Advanced Method for Spectral Fitting (AMARES) within jMRUI (54, 58); 13 ^{31}P multiplets were included (24), assuming Lorentzian line shapes. Shimming variations between experiments were corrected relative to the estimated linewidth of the dominant resonance PCR. Baseline and 2-order phase corrections were performed. For the saturation transfer experiment, the averaged P_i attenuation ratio was calculated as the average ratio of P_i magnetization on γ -ATP saturation M_S over P_i control magnetization M_C for each monkey and each saturation time.

Metabolic modeling and V_{ATP} measurement. The time evolution of P_i longitudinal magnetization can be modeled by using the Bloch equation modified for chemical exchange between P_i and γ -ATP:

$$\frac{dM_{z\text{P}_i}(t)}{dt} = \frac{M_{z\text{P}_i}^0 - M_{z\text{P}_i}(t)}{T_1^{\text{int}}} - k_f M_{z\text{P}_i}(t) + k_r M_{z\gamma\text{ATP}}(t) \quad [3]$$

where $M_{z\text{P}_i}$ and $M_{z\gamma\text{ATP}}$ are the longitudinal magnetizations of P_i and ATP, respectively. $M_{z\text{P}_i}^0$ is the fully relaxed longitudinal magnetization of P_i . P_i attenuation $M_S(t_{\text{sat}})/M_C(t_{\text{sat}})$ depends on the user-fixed sequence parameters (delays t_{OVS} , t_{sat} , and TR, excitation angle θ), and on the following unknown parameters: P_i relaxation time in presence of chemical exchange T_1^{mix} (59), unidirectional rate constant of ATP synthesis k_f , and P_i intrinsic relaxation time in the absence of chemical exchange T_1^{int} (57). T_1^{mix} was estimated by the inversion recovery experiment as previously described. The $M_S(t_{\text{sat}})/M_C(t_{\text{sat}})$ vs. t_{sat} curve was fitted by using a nonlinear least squares algorithm leading to the estimation of the unknown parameters k_f and T_1^{int} . Monte Carlo simulation was also performed on this dataset to assess the accuracy on the 2 fitted parameters. The flux of ATP synthesis V_{ATP} was derived from the equation $V_{\text{ATP}} = k_f[\text{P}_i]$, where the cerebral P_i concentration $[\text{P}_i]$ was estimated from the literature (24–29).

ACKNOWLEDGMENTS. We thank Dr. Luc Pellerin and Dr. Gilles Bonvento for helpful discussion. This work was supported by Java-based MR user interface (jMRUI; <http://www.mruj.uab.es/mruj/>) and the Ministère Délégué à l'Enseignement Supérieur et à la Recherche (Action Concertée Incitative Neurosciences Intégratives et Computationnelles).

- Reivich M, et al. (1977) Measurement of local cerebral glucose metabolism in man with ^{18}F -2-fluoro-2-deoxy-D-glucose. *Acta Neurol Scand Suppl* 64:190–191.
- Kennedy C, Sakurada O, Shinohara M, Jehle J, Sokoloff L (1978) Local cerebral glucose utilization in the normal conscious macaque monkey. *Ann Neurol* 4:293–301.
- Phelps ME, et al. (1979) Tomographic measurement of local cerebral glucose metabolic rate in humans with (F-18)2-fluoro-2-deoxy-D-glucose: Validation of method. *Ann Neurol* 6:371–388.
- Rothman DL, et al. (1985) ^1H -Observe/ ^{13}C -decouple spectroscopic measurements of lactate and glutamate in the rat brain *in vivo*. *Proc Natl Acad Sci USA* 82:1633–1637.
- Mason GF, Rothman DL, Behar KL, Shulman RG (1992) NMR determination of the TCA cycle rate and alpha-ketoglutarate/glutamate exchange rate in rat brain. *J Cereb Blood Flow Metab* 12:434–447.
- Mason GF, et al. (1995) Simultaneous determination of the rates of the TCA cycle, glucose utilization, alpha-ketoglutarate/glutamate exchange, and glutamine synthesis in human brain by NMR. *J Cereb Blood Flow Metab* 15:12–25.
- Mason GF, et al. (1999) Measurement of the tricarboxylic acid cycle rate in human grey and white matter *in vivo* by ^1H - ^{13}C magnetic resonance spectroscopy at 4.1T. *J Cereb Blood Flow Metab* 19:1179–1188.
- Shen J, et al. (1999) Determination of the rate of the glutamate/glutamine cycle in the human brain by *in vivo* ^{13}C NMR. *Proc Natl Acad Sci USA* 96:8235–8240.
- Gruetter R, Seauquert ER, Ugurbil K (2001) A mathematical model of compartmentalized neurotransmitter metabolism in the human brain. *Am J Physiol Endocrinol Metab* 281:E100–E112.
- Chen W, et al. (2001) Study of tricarboxylic acid cycle flux changes in human visual cortex during hemifield visual stimulation using ^1H - ^{13}C MRS and fMRI. *Magn Reson Med* 45:349–355.
- Chhina N, et al. (2001) Measurement of human tricarboxylic acid cycle rates during visual activation by ^{13}C magnetic resonance spectroscopy. *J Neurosci Res* 66:737–746.
- Shoubridge EA, Briggs RW, Radda GK (1982) ^{31}P NMR saturation transfer measurements of the steady state rates of creatine kinase and ATP synthetase in the rat brain. *FEBS Lett* 140:289–292.
- Lei H, Ugurbil K, Chen W (2003) Measurement of unidirectional P_i to ATP flux in human visual cortex at 7T by using *in vivo* ^{31}P magnetic resonance spectroscopy. *Proc Natl Acad Sci USA* 100:14409–14414.
- Zhu XH, et al. (2002) Development of ^{17}O NMR approach for fast imaging of cerebral metabolic rate of oxygen in rat brain at high field. *Proc Natl Acad Sci USA* 99:13194–13199.
- Zhang N, Zhu X-H, Lei H, Ugurbil K, Chen W (2004) Simplified methods for calculating cerebral metabolic rate of oxygen based on ^{17}O magnetic resonance spectroscopic imaging measurement during a short $^{17}\text{O}_2$ inhalation. *J Cereb Blood Flow Metab* 24:840–848.

